Short Communication

Application of Electrochemical Impedance Spectroscopy to Evaluate the Corrosion Behavior of 2304 Duplex Stainless Steel Reinforced Rebar in Concrete Exposed in Chloride-Rich Environment

Wu Zhao[1], Jianguo Zhao[2], Shengjing Zhang[2], Jinbo Yang[1,]*

[1] College of Water Conservancy and Civil Engineering, Shandong Agriculture University, Taian, 271000, China.
[2] Shandong Luzhu Cement Co. Ltd., Taian, 271400, China.
[*]E-mail: yangjinbo@tsinghua.org.cn and yangjinbotsinghua@aliyun.com

Corrosion of steel bars embedded in concrete is one of the main causes affecting the long-term performance of reinforced concrete structures. In this study, the corrosion behavior of AISI 2304 stainless steel reinforced calcium silicate cement concrete in chloride-rich environments were evaluated by electrochemical impedance spectroscopy (EIS). The EIS results show that both the immersion time and pH play significant roles in the evolvement of the charge transfer processes and film resistance. At pH value of 13, the total impedance increased during the 3 months of immersion time, and then it slightly reduced, indicating the protective ability is being lost. The calcium silicate concrete with steel rebar indicated that the samples remained in the passive state throughout the linear polarization resistance test. The polarization resistance value attained in the pH solutions of 13 are upper than that in other pH values which show higher capability for corrosion prevention in the pH value of 13.

1. INTRODUCTION

The corrosion process in reinforced concrete structures regularly leads to serious damages that reduces the service life of structures [1]. Various factors are effective in this destruction, such as the compactness, proportions of the contents, the thickness and the homogeneity of the concrete, environmental humidity and the reinforcement surface condition [2]. Moreover, the interference currents, existence of mechanical stresses in steel, galvanic contact between two different metals,

atmospheric CO_2, the existence of aggressive ions (such as Cl^-, SO_4^{2-}) or any alkaline neutralizing fluid may be the cause of the metal deterioration [3-8].

Steel reinforced concrete are extremely corrosion-resistant structures, because the alkali environments passivate the steel by creation of an Iron (III) oxide-hydroxide layer [9]. However, steel reinforced concrete may deteriorate when many corrosion products are created on the steel. The presence of moisture and Cl^- ions can lead to breakdown of the passive film and localized corrosion. The utilization of stainless steels is an alternative method in reinforced concrete structures for long useful life or for working in extremely aggressive environments. Recently, there is no serious risk for increasing the rate of galvanic corrosion when carbon steel and stainless steel embedded in concrete. However, the use of stainless steel is expensive at first, saves costs in the long term, removing rebar coatings, concrete sealers, cement inhibitors, maintenance costs, etc. [10, 11]. Three main types of stainless steel, austenitic, ferritic and ferritic–austenitic (duplex) are appropriate to produce rebar reinforcement with various properties.

Although calcium silicate hydrate is very important for strength and durability of cement paste, numerous ambiguities remain about its atomic structure. This information is critical for optimizing calcium silicate-based concretes with the purpose of decreasing the CO_2 related with its production. Despite wide research, the study on calcium silicate cements continued to analyze direct atomic structure for two chief reasons: its broad diffraction signal and difficulty in phase separation. The production of each ton of Portland clinker released about 0.8 tonnes of CO_2 in the atmosphere, containing 5%–7% of the total human-made CO_2 emissions.

Diffusion of chloride ions in concrete is slow and complex. Although many approaches have been reported to estimate chloride diffusion coefficients in the literature [12-16], not much data is available for reinforced concrete. Here, the influence of chloride ions in reinforced calcium silicate concrete and effect on corrosion behavior of stainless steel were investigated.

Although many researches have been reported on calcium silicate concrete, studies associated to EIS measurements of reinforced calcium silicate cement concrete are still limited. In this study, a duplex stainless steel was used to make reinforcing bars, recognized as stainless steel grade duplex 2304. Furthermore, the corrosion behavior of AISI 2304 stainless steel reinforced calcium silicate cement concrete in chloride-rich environments were evaluated by EIS.

2. MATERIALS AND METHOD

Stainless steel grade Duplex 2304 was used in this study that is a balance of austenitic and ferritic. The chemical composition of stainless steel is defined in Table 1.

Table 1. Chemical composition of AISI 2304 Stainless Steel bar.

Element	Content (%)
Iron, Fe	72.679
Nickel, Ni	4
Chromium, Cr	23
Molybdenum, Mo	0.20
Carbon, C	0.02
Nitrogen, N	0.1
Sulfur, S	0.001

Steel bars were cleaned with silicon carbide paper and then washed with water and ethanol. The chemical composition of the Portland cement as calcium silicate binders is summarized in Table 2.

Table 2. chemical composition of the Portland cement as calcium silicate binders

Compositions	Contents (wt%)
CaO	63.1
SiO_2	19.8
Al_2O_3	4.9
Fe_2O_3	2
MgO	2
SO_3	3.8
Blaine (m^2/kg)	373
LoI	1.8

The calcium silicate cement was made by the mixture of 45 wt% Clay/Shale/Sand and 55 wt% Limestone at furnace temperature of 1200 ˚C by 3.8 Gj energy/t and 550 kg CO_2/t of cement. Mortar was made using calcium silicate cement with 0.5 water/cement ratio. Concrete cylinder were constructed with a similar proportion that had gravel, sand and cement with the ratio of 4:2:1. The radius and height of prepared concrete cylinder are 40 mm and 110 mm, respectively. The steel reinforced concrete specimens were located at an environmental chamber at room temperature to precipitate the corrosion procedure of the carbon steel bar. pH of electrolyte solution varies with changes in the concentration of the solution composition, so that a reduction in salt concentration results a decrease in Ph of electrolyte solution. Specimens for corrosion study were immersed into corrosive environment including a 0.1 M NaOH, 0.01 M Ca(OH)$_2$ and 0.1 M KOH with pH ranging from 10 to 13. The 0.3 M Cl concentration was added to the solution. Evaluations were periodically performed after 1, 2, 3, 4 and 5 months of exposure. EIS characterizations were performed in the frequency varied between 100 kHz and 0.1 mHz at the E_{OC} with AC perturbation ±10 mV.
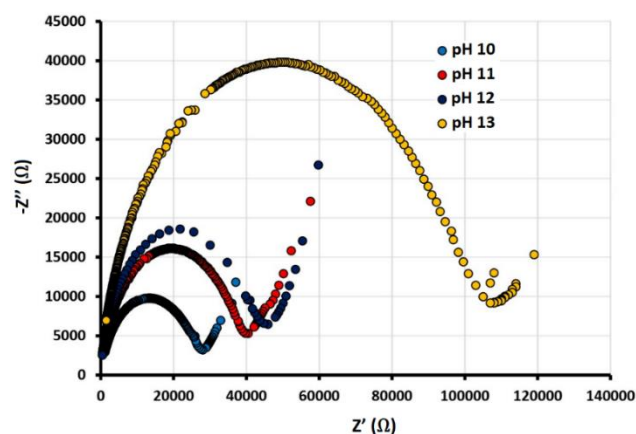
3. RESULTS AND DISCUSSION

Figure 1. Nyquist diagrams of 2304 duplex stainless steel rebar immersed into different pH solution at room temperature and 1 month immersion time

Figure 1 shows the Nyquist diagrams of 2304 duplex stainless steel immersed into different pH solution which indicted a capacitive arc at low frequency. As shown in the figure 1, the capacitive arc radius increases with increasing pH values. In the EIS measurement, the semi-circular arc radius is associated to the polarization resistance (R_p) of the passive film [17]. an enhancement in the overall impedance values at pH value of 13 reveals an increase of the corrosion resistance that is in good agreement with th
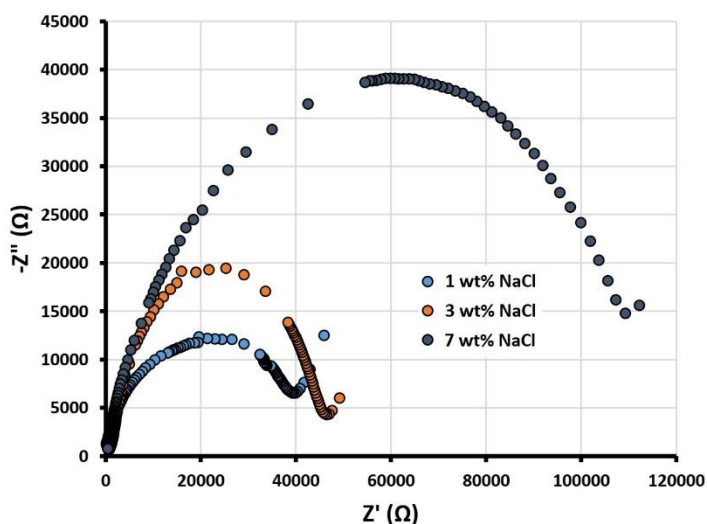
e previous studies.

Figure 2. Nyquist diagrams of stainless steel rebar immersed into different concentration of NaCl in chloride-rich environments at room temperature and 1 month immersion time
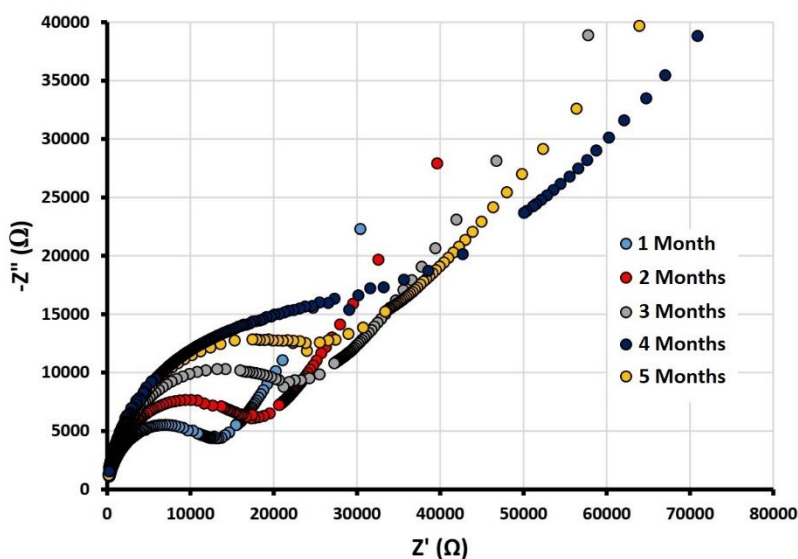

Figure 3. Nyquist plots of 2304 duplex stainless steel rebar in chloride-rich environment with pH 10 after different exposure times at room temperature

Figure 2 shows the the Nyquist diagrams of stainless steel rebar immersed into different concentration of NaCl in chloride-rich environments. One loop of the graph represents the corrosion reactions under charge transfer control. As shown in the figure 2, by increasing NaCl concentrations into electrolyte solution, the polarization resistance was enhanced. Furthermore, the reduction of corrosion rate was illustrated due to absorbtion of Cl ions on the surface of rebar. As a results, corrosion rate reduced by increasing the value of salinity.
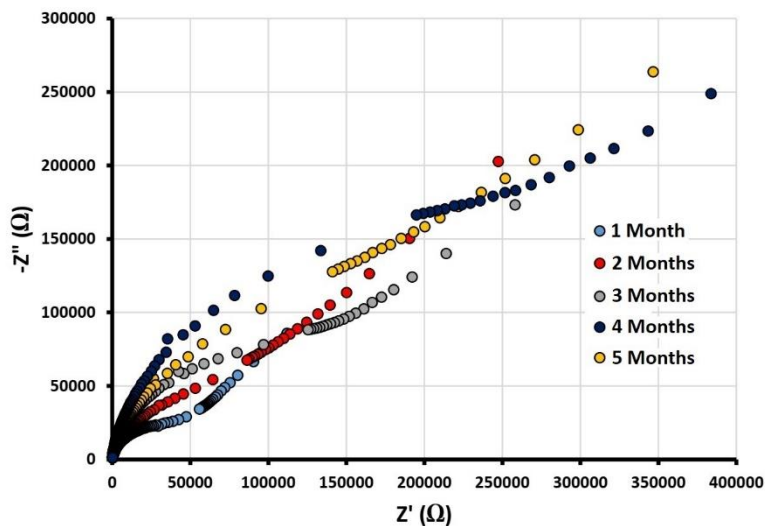

Figure 4. Nyquist plots of 2304 duplex stainless steel rebar in chloride-rich environment with pH 13 after different exposure times at room temperature

In order to describe corrosion behavior of the stainless steel reinforced concrete and immersed to the chloride environment, EIS spectra were performed after different exposure times. The impedances of open-circuit in the stainless steels were outlined over 4 months from the sample immersion into the alkaline solution with 10 and 13 pH value. The immersion time effect on the experimental spectra is indicated in figures 3 and 4 as a Nyquist plots. The investigation of the total impedance reveals higher values of arc radius with increase of the immersion time, indicating a development of passive layer and an enhancement of protection behavior of 2304 duplex stainless steel in the test environment. At pH value of 13, the total impedance increased during the 3 months of immersion time, and then it slightly reduced, indicating the protective ability is being lost (Figure 4). At pH value of 10, the impedance started to reduction after 3 months of immersion time, showing the surface of steel bars are more sensitive to pitting attack. Therefore, Reducing the pH values from 13 to 10 causes the surface to become more sensitive to Cl^- ions attack.
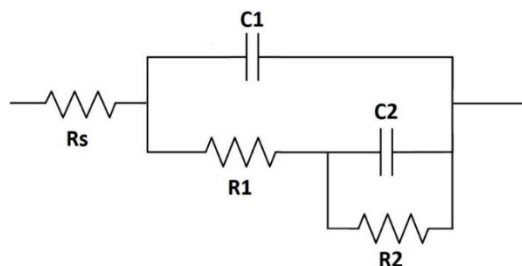
Figure 5. An equivalent circuit model to fit the experimental data

Different models have been proposed for the interpretation of impedance spectrum on the passive metal surface. As mentioned in the literature [18-20], an equivalent circuit as shown in Figure 5 was accepted to fit the experimental results. This model assumes that the passive layer does not completely cover the metal surface and cannot be measured as a homogeneous layer. Actually, neither of these, active surfaces of solids and passive layers on metallic substrates cannot be considered as ideal homogeneous. As shown in Figures 1-4, there is a good accordance between the equivalent circuit calculations and the experimental data.

Polarization resistance (Rp) is usually used to measure the metal resistance in the corrosion damage.

$$Rp = R_1 + R_2 \tag{1}$$

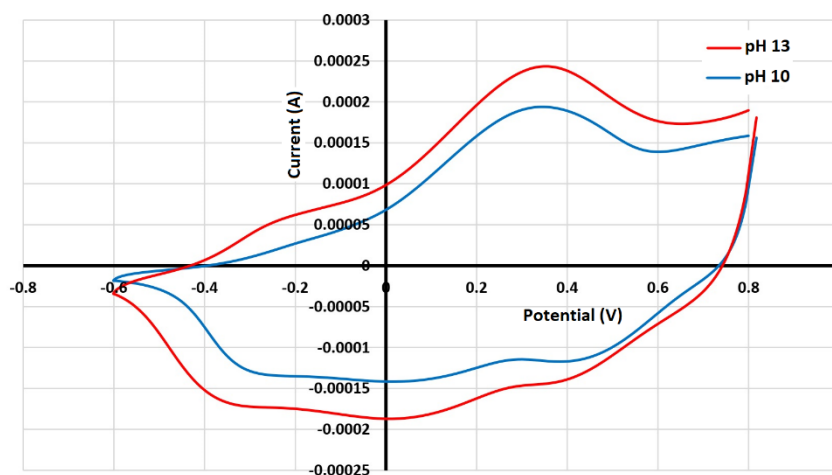where R_1 and R_2 values are parameters of the fitting procedure.

Figure 6. CV scans of the passivation film formation on steel rebar at pH condition 10 and 13

Figure 6 shows the cyclic voltammetry (CV) results of passivation films formation on rebar surface at pH values of 10 and 13. Peak shifts were clearly observed on the CV curves when the pH value decreasing, which is in a good accordance with the Pourbaix diagrams explanation [21]. Furthermore, the peak intensities also indicated decline, suggesting the degree of the formed passivation film reduced at the lower pH condition. Consequently, the magnetite formation was less

effective under low pH conditions. The observation was in good accordance with other reports [22, 23].

Figure 7 shows the effect of immersion time on the Rp value in the various pH of solutions. At the initial immersion time, the polarization resistance is small and reaches to 1.2 MΩ after 2 months' immersion at pH value of 10, then it tends to stay stable. After the immersion for over 4 months, it slightly reduced. In all samples, Rp values attained in the pH solutions of 13 are upper than that in other pH values which show higher capability for corrosion prevention in the pH value of 13 [24].
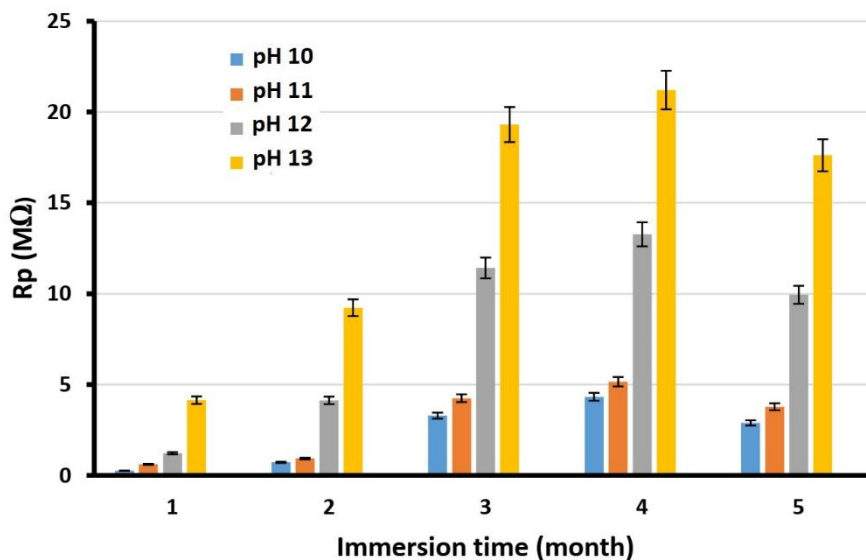

Figure 7. Polarization resistance of 2304 duplex stainless steel rebar in chloride-rich environment with different pH values after different exposure times at room temperature
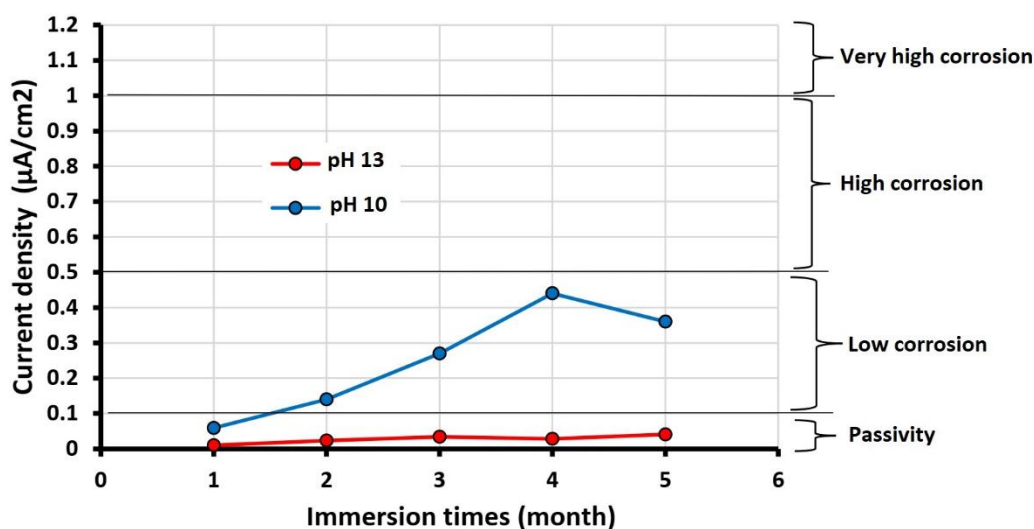

Figure 8. The time-dependent changes of corrosion current density for steel rebar with 10 and 13 pH values after different exposure times at room temperature

Figure 8 indicates the time-dependent changes of corrosion current density through the liner polarization resistance tests. The corrosion level can be defined into four levels proposed by Durar Network Specification [25]: very high corrosion for $1.0 \ \mu A/cm^2 < i_{corr}$, high corrosion for $0.5 \ \mu A/cm2 < i_{corr} < 1.0 \ \mu A/cm^2$, low corrosion for $0.1 \ \mu A/ \ cm^2 < i_{corr} < 0.5 \ \mu A/cm^2$, and passivity for $i_{corr} < 0.1 \ \mu A/cm^2$. Mortar cylinders with stainless steel rebar at environment pH value of 10 experienced only two states: passive state at the initial of immersion procedure and low corrosion after 2 months of immersion times. Steel reinforced concrete at environment pH value of 13 remained completely in the passive state during the test. Therefore, the reinforced concrete at pH solution of 13 has a lower corrosion current density than that at pH solution of 10.

4. CONCLUSIONS

The corrosion process in reinforced concrete structures regularly leads to serious damages that reduces the service life of structures. In this research, the corrosion behavior of 2304 duplex stainless steel reinforced calcium silicate cement concrete in chloride-rich environments were evaluated using EIS technique. Nyquist diagrams of reinforced concrete immersed into different pH solution indicted a capacitive arc at low frequency. The impedances of open-circuit in the stainless steels were outlined over 4 months from the sample immersion into the alkaline solution with 10 and 13 pH value. At pH value of 13, the total impedance increased during the 3 months of immersion time, and then it slightly reduced, indicating the protective ability is being lost. Steel reinforced concrete at environment pH value of 13 remained completely in the passive state during the test. Furthermore, the reinforced concrete at pH solution of 13 has a lower corrosion current density than that at pH solution of 10.

References

1.   P. Zhang, Y. Cong, M. Vogel, Z. Liu, H.S. Müller, Y. Zhu and T. Zhao, *Construction and Building Materials*, 148 (2017) 113.
2.   Z. Jin, X. Zhao, T. Zhao and L. Yang, *International Journal of Electrochemical Science*, 11 (2016) 8779.
3.   W. Li, B. Pots, X. Zhong and S. Nesic, *Corrosion Science*, 126 (2017) 208.
4.   X. Y. Min, X. Wu, P. H. Shao, Z. Ren, L. Ding, X. B. Luo, *Chem. Eng. J.,* 358 (2019) 321.
5.   H. Y. Yu, P. H. Shao, L. L. Fang, J. J. Pei, L. Ding, S. G. Pavlostathis and X. B. Luo, *Chem. Eng.J.*, 359 (2019) 176.
6.   S. F. Tang, D. L. Yuan, Y. D. Rao, M. H. Li, G. M. Shi, J. M. Gu and T. H. Zhang. *J. Hazard. Mater.*, 366 (2019) 669
7.   L.M. Yang, Z.L. Chen, D. Cui, X. B. Luo, B. Liang, L.X. Yang, T. Liu, A. J. Wang and S. L. Luo. *Chem. Eng. J.,* 359(2019)894.
8.   J. Rouhi, S. Mahmud, S. Hutagalung and N. Naderi, *Electronics letters*, 48 (2012) 712.
9.   M. Liu, X. Cheng, G. Zhao, X. Li and Y. Pan, *Surface and Interface Analysis*, 48 (2016) 981.

10. F. Lollini, M. Carsana, M. Gastaldi and E. Redaelli, *Corrosion Reviews*, 37 (2019) 3.
11. S. Kakooei, H.M. Akil, M. Jamshidi and J. Rouhi, *Construction and Building Materials*, 27 (2012) 73.
12. T. Zhang and O.E. Gjørv, *Cement and Concrete Research*, 24 (1994) 1534.
13. K. Ann, J. Ahn and J. Ryou, *Construction and Building Materials*, 23 (2009) 239.
14. S. Kakooei, H.M. Akil, A. Dolati and J. Rouhi, *Construction and Building Materials*, 35 (2012) 564.
15. Q. Sun, Y. Yang, Z. Zhao, Q. Zhang, X. Zhao, G. Nie, T. Jiao and Q. Peng, *Environ. Sci: Nano*, 5(2018) 2440.
16. M.Green, A.T.V.Tran, R. Smedley,Adam. Roach, J. Murowchick, X.B.Chen, *Nano Materials Science.48(2019)*.
17. H. Luo, H. Su, C. Dong and X. Li, *Applied Surface Science*, 400 (2017)
18. B. Guitián, X. Nóvoa and B. Puga, *Electrochimica Acta*, 56 (2011) 7772.
19. H. Luo, C. Dong, K. Xiao and X. Li, *Applied surface science*, 258 (2011) 631.
20. A. Kocijan, D.K. Merl and M. Jenko, *Corrosion Science*, 53 (2011) 776.
21. X. Shang, Y. Zhang, N. Qu and X. Tang, *International Journal of Electrochemical Science*, 11 (2016) 5870.
22. L. Freire, M. Carmezim, M.a. Ferreira and M. Montemor, *Electrochimica Acta*, 55 (2010) 6174.
23. L. Freire, M. Carmezim, M. Ferreira and M. Montemor, *Electrochimica Acta*, 56 (2011) 5280.
24. S. Zhang, Q. Lu, Y. Xu, K. He, K. Liang and Y. Tan, *International Journal of Electrochemical Science*, 13 (2018) 3246.
25. R. Galván-Martínez, C. Gaona-Tiburcio and F. Almeraya-Calderón, *International Journal of Electrochemical Science*, 11 (2016) 2994.